RESULTS FROM THE LUMINOSITY OSCILLATIONS IMAGER

T.Appourchaux[1], T.Toutain[2], A.Jiménez[3], M.C.Rabello Soares[3], B.N.Andersen[4] and A.R.Jones[5]

[1] Space Science Department of ESA, ESTEC, NL-2200 AG Noordwijk, (thierrya@so.estec.esa.nl)
[2] Observatoire de la Côte d'Azur, F-06003 Nice Cedex, (toutain@obs-nice.fr)
[3] Instituto de Astrofisica de Canarias, Universidad de La Laguna, E-38071 La Laguna, Tenerife, (ajm@iac.es)
[4] Norwegian Space Centre, N-0309 Oslo 3, (bo@admin.nsc.no)
[5] Bartol Research Institute, 950 N. Cherry Avenue, P. O. Box 26732, Tucson, Arizona 85719, (jones@cyprus.spole.gov)

ABSTRACT

The Luminosity Oscillations Imager is a part of the VIRGO instrument to be flown aboard the Solar and Heliospheric Observatory (SOHO) in mid 1995. Using a ground-based version of the instrument, we have detected low-l modes with 2 time series spanning 163 days each (from May 2 to October 11, 1994; and from September 17, 1994 to February 26, 1995). The low resolution capability of the instrument allows the identification of individual tesseral orders for l=2 to 5. The data reduction method prevents from observing the l=0 modes, and reduces the amplitude of the l=1 modes with $m = \pm 1$. For each time series, the frequencies and the linear component (a_1) of the mode splitting are given for l=2 to 5 for each order n. The frequencies and the a_1 are obtained by fitting simultaneously the $2l$+1 spectra with maximum likelihood estimators. The splittings are compared with other published values.

Keywords: solar oscillations - p modes - internal rotation

1. Introduction

Helioseismology is a powerful tool to infer the internal structure of the sun. Over the last two decades several groups, using various apparatus, reported on the detection of global solar p modes. High resolution imaging instruments can detect degree down to l=3 (Harvey, 1988) while separating the individual tesseral orders m, allowing us to measure the splitting of the modes. Unfortunately the instability of these instruments prevents to reliably detect modes with $l < 3$. Integrated sunlight instruments do not have any resolution, but they can detect degrees from l=0 to l=3 (Harvey, 1988). The various m components are not all detected and are mixed in the power spectra, making the determination of mode splitting at low l difficult. Various attempts to measure those splittings are starting to give consistent results (Jiménez et al, 1994; Loudagh et al, 1993; Toutain and Kosovichev, 1994). Nevertheless, the rotational splitting given by these authors is an average over various n and l.

Recently, Tomczyk et al (1994) reported on the observation of the splitting of low-l modes using an imaging instrument with a very stable zero point. Their work pushed us to detect also the splittings of these modes with the Luminosity Oscillations Imager (LOI). The LOI was built by the Space Science Department of the European Space Agency as a contribution to the VIRGO instrument. After the completion of the flight programme, we installed in May 1994 the Qualification Model of the LOI at the Observatorio del Teide (Izaña, Tenerife) for detecting in intensity low-l p modes. Due to the atmospheric noise, the detection of p modes in intensity is difficult (Jiménez et al, 1987; Andersen and Domingo, 1988). Nevertheless, the successful observation of low-l p modes by the LOI contributes to the determination of the rotational splitting of low-l modes; this was already reported by Appourchaux et al (1995). Here we present newer results with the analysis of two quasi independent time series: one from May 2, 1994 to October 11, 1994 (same as in Appourchaux et al, 1995), and one from September 19, 1994 to February 26, 1995. The frequencies and the a_1 component of the splitting are given for each n and l, for both time series.

In this article firstly we browse the LOI instrument (a more detailed description can be found in these proceedings). In the second part the data reduction analysis is developed. In the third section, we expose how the spectra were analysed. In the fourth section, we compare our splittings with other available values and then conclude.

2. Description of the LOI instrument

The design of the LOI instrument was an original idea of Andersen et al (1988). The instrument is described in details in these proceedings (Appourchaux et al, 1995). It consists of a Ritchey-Chrétien telescope (f=1300 mm) imaging the sun through a 5-nm passband interference filter at 500 nm. The image is projected on a photodiode array detector built to our specifications (Appourchaux et al, 1992). The detector is made out of 12 scientific pixels and of 4 guiding pixels. The shape of the scientific pixels are optimized to detect low degree modes for $l < 7$ (Appourchaux and Andersen, 1990). The guiding pixels are 4 quadrants of an annulus with an inner and outer radius of 0.95 and 1.05 solar radius, respectively. The error signals for the guiding servo are the differences between two opposite pixels. The error signals are fed back to two piezoelectric actuators that move the secondary mirror around its vertex. The actuators provide both the coarse and fine pointing; the total range of the Qualification Model is ±5' with a 0.2" precision; the 3db bandwidth of the servo control is 10 Hz. The current of each scientific pixel is amplified and digitised using Voltage-to-Frequency Converters (VFCs). The current of each guiding pixel is amplified and digitised using A/D converters. The 12 scientific pixels are read simultaneously while the 4 guiding pixels are read sequentially. The sampling time of the instrument is 53.687523 s. The integration time of the scientific pixels is about 99% of the sampling time. The housekeeping integration time of the guiding pixels is about 2 s. The instrument is controlled with a PC and all scientific and housekeeping data are stored on a hard disk.

3. Observations

The LOI instrument was installed on an equatorial mount on May 2, 1994 in Tenerife. The observations analysed

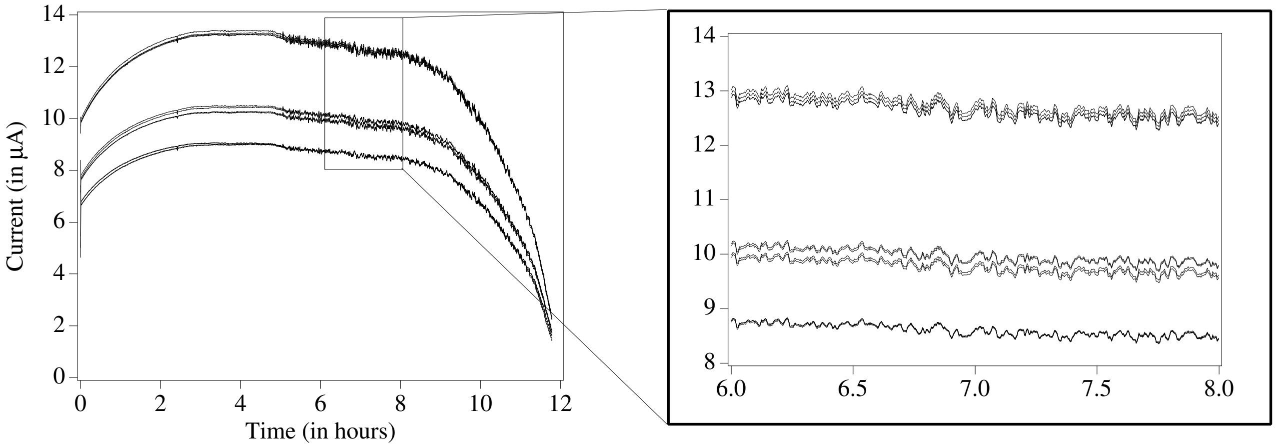

Figure 1: A typical day of observation: left, the current of the 12 pixels as a function of time; right, an enlargement shows that the atmospheric fluctuations are coherent over the sun.

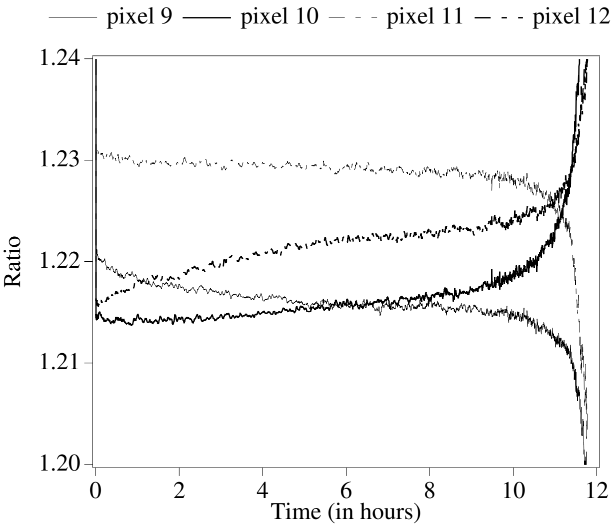

Figure 2: Ratio of the central pixels to the average as a function of time. The effect of the differential extinction is obvious at the end of the day.

here starts from May 2, 1994 and ends on February 26, 1995. The duty cycle is about 33% over 10 months. During the 10 months of operations, the instrument had not a single failure; only 2 days were lost due to a parity error in the PC. The instrument is easy to set everyday: it requires only to be aligned on the sun in the morning, and everything thereafter is automatic. The clock of the PC drifts from day to day. This drift is daily measured and if necessary the PC clock is readjusted. The observed stability of the guiding was about 0.2-0.4". This is an upper limit since the atmospheric transparency changes as the guiding pixels are read. The LOI was not aligned with the solar rotation axis and the sun was rotating from day to day with respect to the detector.

4. Data reduction

4.1 Correction of atmospheric effects

It is well known that the fluctuations of the atmospheric transparency is the prime source of noise for detecting the p modes in intensity. But thanks to the coherence of the atmosphere, the effect is the same for the 12 pixels of the instrument as can be seen on Figure 1. The first order correction of the atmospheric transparency is performed by dividing each pixel by an average over the 12 pixels, This reduces by about a factor 20 in the worst case the atmospheric noise.

4.2 Correction of differential extinction and pixel sensitivity

After the first correction, there are still low frequency variations due to the different zenithal distances sampled by the pixels. This effect is clearly seen in Figure 2 for the central pixels. For correcting for these variations, we compute the residuals using a running mean which is a gaussian filter with a frequency cut-on of 0.5 mHz. This also takes care of correcting the difference in the sensitivity of the pixels. The result is shown in Figure 3. For each pixel, the lowest σ of the series is used to remove spikes greater than 5σ; the spikes are replaced by zeros. The last step is to synchronise, every day, the time series for each pixel using a linear interpolation. No other instrumental correction are performed. These data are used for computing the time series for a given l, m mode.

4.3 Optimal filtering for mode extraction

The optimal linear combination of the pixels to obtain a given l, m mode was reported by Appourchaux and Andersen (1990). Since the sun rotates with respect to the detector (the P and B angles are not negligible) the optimal filters are updated every week and a linear interpolation provide the daily optimal filter. If one were to neglect this image rotation, one would see the effect by an increased cross talk between the modes. In a previous paper (Appourchaux et al, 1995), we used the optimal filters computed for a perfect LOI detector. Since then, we have updated our filters taking into account the real configuration of the flight detector, and also correcting for an error in the orientation of the sun on the detector; this latter led us to underestimate the splitting in the paper (Appourchaux et al, 1995).

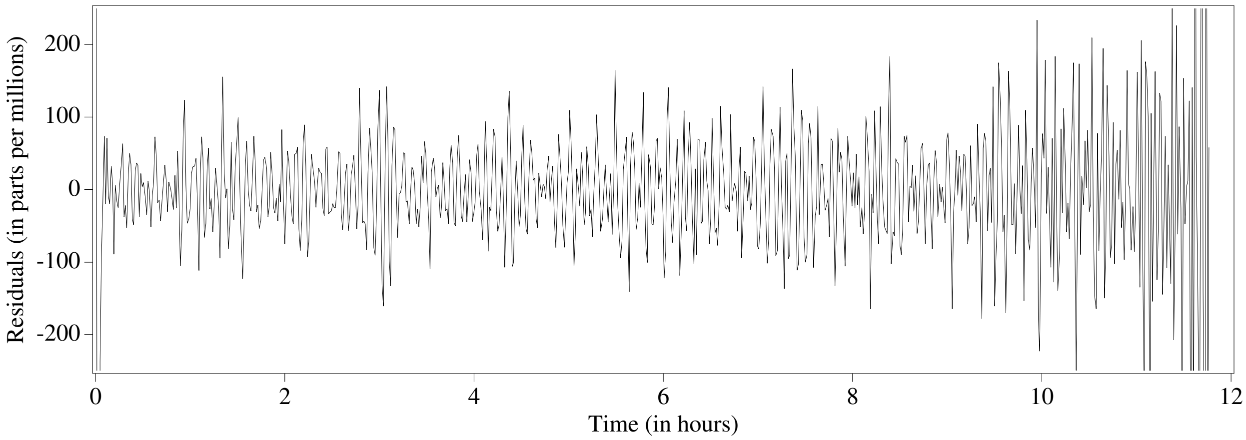

Figure 3: Residuals for the pixel 12 after removing the low frequencies using a running mean filter. The 5-min oscillations are clearly visible. It can be noticed that although the atmosphere is much less quiet after the 5th hour (see Figure 1), the fluctuations have the same peak-to-peak amplitude. This is because the coherence size of the atmosphere does not during the day. The coherence is only lost at the end of the day.

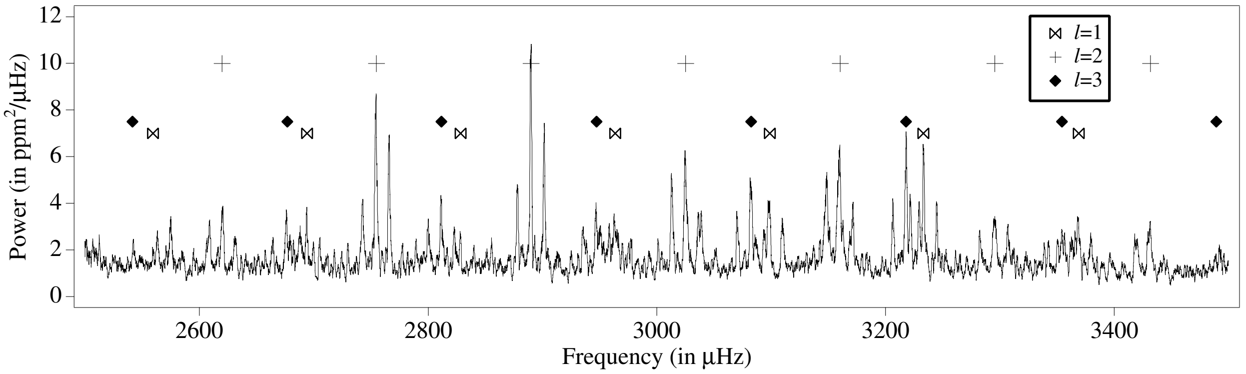

Figure 4: Power spectrum for the $l = 1, m = 0$ optimal filter, smoothed to 21 points to enhance the modes. The frequency resolution is 0.071 μHz. Each mode and its two aliases can be identified. In addition, the spatial sidelobes are clearly visible; they are the $l = 2, m = \pm 1$, and the $l = 3, m = 0$ modes.

4.4 Time series and power spectra

For the l, m mode to be analysed, a single time series is obtained by computing the weighted average over the 12 pixels using the optimal filter of the l, m mode. The optimal filters are complex and allow us to separate the prograde and retrograde modes in the Fourier space. To minimise the atmospheric noise, the time series for the given l, m mode are weighted by the daily variance; this provides a significant improvement in the power spectra. The time series are normalised to take into account the weighted window function. The frequency resolution of the power spectra is 0.071 μHz.

Figure 4 shows the power spectrum for the l=1, m=0 optimal filter; modes with l=1, 2 and 3 are clearly detected with amplitudes of about a few part-per-million (ppm). The noise level is about 0.8 ppm$^2/\mu$Hz which is about a factor 4 higher than the noise obtained from space by IPHIR. The signal-to-noise ratio in the power spectra ranges from 1 to 4. It must be pointed out that contrary to what has been reported by Pallé et al (1993), the l=1, m=0 modes are detected by Tomczyk (1994) and by us. The data reduction procedure prevents us from detecting the l=0 mode because this mode is filtered out when correcting for the fluctuations of the atmospheric transparency. For the same reason the l=1, $m = \pm 1$ modes are attenuated by a factor of 4 in the power spectrum. In addition these modes are mixed in the power spectra because their relative phases are lost in the process.

Figure 5 shows an $m - \nu$ diagram for two l=2 and $l = 3$ modes.

5. Frequencies and splittings

In order to extract in the best way the information contained in the spectra, we chose to fit simultaneously the $2l$+1 spectra of a given n, l mode using maximum likelihood estimators (MLE); this technique is also used by Tomczyk et al (1994). The window for the MLE was 14.2 μHz centred on the frequency of the m=0 mode. We assumed that the linewidth is the same for the $2l$+1 components of an n, l mode; and that the frequency of an m component is ν_m=ν_0 + ma_1, where a_1 is the linear component of the splitting. The maximum likelihood technique is well known and its error propagation properties are well understood (Toutain and Appourchaux, 1994). The use of MLE leads to two major approximations. Firstly, it is assumed that in a power spectrum the frequency bins are independent of each other. This

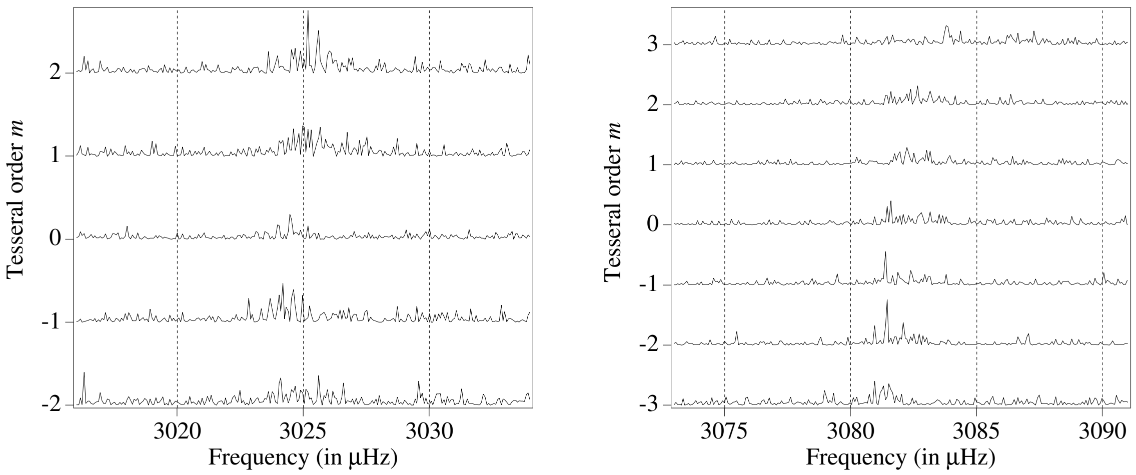

Figure 5: $m - \nu$ diagram for typical l=2 (left) and l = 3 (right) modes. The spectra are not smoothed. The rotational splitting can be easily seen.

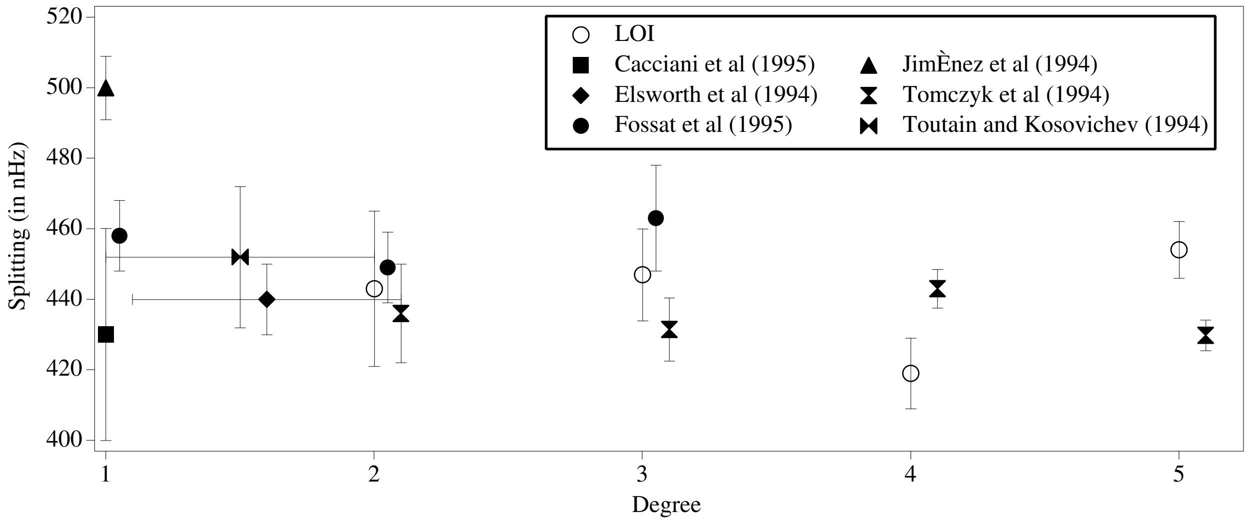

Figure 6: Splitting as a function of l as measured by various authors. The LOI values are an average over the two 5-month time series. All splitting error bars are 1-σ value. Error bars associated with the degree indicate an average over l.

is not true as we have gaps in the data (Gabriel, 1994). Nevertheless, the method we used is much simpler than the method suggested by Gabriel (1994), and will not bias the estimate on frequency (Lazrek and Hill, 1992) and splittings. Secondly, we assumed that for a given l, the $2l$+1 spectra are independent of each other. This is a very good approximation even if there is a crosstalk (due to the imperfect isolation of a given l,m mode) between the $2l$+1 spectra. The effect of the crosstalk is to couple for a given n, l mode the m components with each other; this was taken into account in the analysis. Due to the small correlation between the $2l$+1 spectra, the error bars on the frequency and splitting will be slightly underestimated. The same underestimation happens if one uses the temporal sidelobes at 11.57 μHz: the error bars would be underestimated by about a factor $\sqrt{3}$. Due to the low signal-to-noise ratio in our spectra, we believe that a slight improvement in our frequencies and splittings could be obtained by adding the temporal sidelobes; it is yet to be done. The correct treatment of the power spectra taking into account the statistical dependencies (frequency bins, temporal and spatial sidelobes) remain to be done using the method described by Gabriel (1994). However we believe that only the estimate of the error bars on the frequency and splitting are biased, and not the values themselves. To minimise this bias, the error bars have been corrected at least from the crosstalk between the various m components. Tables 1, 2 and Tables 3, 4 summarise, respectively the frequencies and the splittings of the detected modes for both time series. In addition, an optimal weighted average ($<>$) of a_1 is given in Tables 3 and 4.

6. Splitting comparison

We must first point out that now our splittings are not systematically lower than other published values. One of the goals of this paper was to find out why our splittings had such a behaviour in a previous paper (Appourchaux et al, 1995). An error in the orientation of the sun on the detector was found that explained very well the systematic error. The sun was upside down on the detector which led to additional crosstalk in a given l, m spectrum from modes with $\Delta m = \pm 1$; this crosstalk was not modelled since it should be null to the first order. This additional power pulled down the estimate of the splitting.

Figure 6 shows a comparison of splittings measured by various authors. It becomes clear now that the splittings of very low degree modes do not display any dramatic change from the surface value. The values quoted by Elsworth et al (1994), Toutain and Kosovichev (1994), Tomczyk et al (1994) and now by Fossat et al (1995), and by Cacciani et al (1995) (both these proceedings) are in good agreement with our results.

Corbard et al (1995) (these proceedings) used the LOI splittings to infer the rotation inside the sun. For $l > 4$, they used the BBSO splittings (Libbrecht and Woodard, 1993). They found the same results as of Tomczyk et al (1994): that is the sun rotates with a flat rate below the convection zone down to 0.2 $R_{\odot}$. Of course the results is not surprising given the splitting we have. More accurate rotation inversion are obtained with an homogenous data set such as the one of Tomczyk et al (1994).

7. Conclusion

Against all odds, we have shown that the very low degree modes could be detected in intensity from a ground-based observatory. It permitted us to do some useful new science, and also to validate the design of the LOI before the launch of SOHO. We are now confident that we will be able to detect the g modes with the LOI. We are now looking forward to the launch of this satellite.

Acknowledgement. We are very grateful to the many observers of IAC who operated with dedication the LOI instrument during all these months. We are also grateful for the many discussions we had at the workshop with Gabrielle Berthomieu, Yvonne Elsworth, Eric Fossat, Douglas Gough, Janine Provost and Steve Tomczyk. One of the authors (TA) would like to thank Judy and Steve for their kind hospitality and comprehension during his stay in Boulder. The useful comments of Bernhard Fleck on an erlier version of the paper were very much appreciated.

REFERENCES

1. Andersen, B.N. and Domingo, V., IAU Symposium 123, J.Christensen-Dalsgaard and S.Frandsen eds, Reidel, p. 67
2. Andersen, B.N, Domingo, V., Jones, A.R. et al, 1988, ESA SP-286, Eds V.Domingo and E.J.Rolfe, p. 385
3. Appourchaux, T. and Andersen, B.N., 1990, Sol.Phys. 128, 91
4. Appourchaux, T., Martin, D. and Telljohann, U., 1992, SPIE 1679, 200
5. Appourchaux, T., Toutain, T., Telljohann, U., Jiménez, A., Rabello-Soares, M.C., Andersen, B.N. and Jones, A.R., 1995, A&A 294, L13
6. Elsworth, Y., Howe, R., Isaak, G.R. et al, 1994, To appear in the proceedings of the GONG-94 conference
7. Gabriel, M., 1994, A&A 287, 685
8. Harvey, J., 1988, ESA SP-286, Eds V.Domingo and E.J.Rolfe, p. 55
9. Jiménez, A., Pallé, P.L., Roca Cortés, T. et al, 1987, A&A 172, 323
10. Jiménez, A., Perez Hernandez, F., Claret, A. et al, 1994, ApJ 435, 874
11. Lazrek, M. and Hill, F., 1992, A&A 280, 704
12. Libbrecht, K.G. and Woodard, M., 1993, Compilation of p-mode data, Big Bear Solar Observatory, available via the World Wide Web: ftp://helios.tuc.noao.edu/pub/bbso
13. Loudagh, S., Provost, J., Berthomieu, G. et al, 1993, A&A 275, L25
14. Pallé, P.L., Perez Hernández, F., Régulo, C. and Roca Cortés, T., 1993, ASP Conference Series 42, p. 189
15. Tomczyk, S., Schou, J. and Thompson, M.J., 1994, submitted to ApJ Letter
16. Toutain, T. and Appourchaux, T., 1994, A&A 289, 649
17. Toutain, T. and Kosovichev, A., 1994, A&A 284, 265

Table 1: Frequencies and 1-σ error in (μHz) of low-l p modes for the time series spanning May 2 to October 11, 1994 as measured by the LOI.

n	l=2	l=3	l=4	l=5
15	-	2408.23 $\pm$ 0.23	2459.04 $\pm$ 0.16	2505.94 $\pm$ 0.18
16	2485.59 $\pm$ 0.23	2541.83 $\pm$ 0.12	2593.08 $\pm$ 0.16	2641.59 $\pm$ 0.14
17	-	2676.55 $\pm$ 0.21	2728.62 $\pm$ 0.15	2777.08 $\pm$ 0.11
18	2754.41 $\pm$ 0.12	2811.57 $\pm$ 0.08	2864.05 $\pm$ 0.07	2913.52 $\pm$ 0.12
19	2889.88 $\pm$ 0.07	2946.95 $\pm$ 0.07	3000.25 $\pm$ 0.10	3049.80 $\pm$ 0.10
20	3024.76 $\pm$ 0.10	3082.36 $\pm$ 0.13	3135.95 $\pm$ 0.09	3186.13 $\pm$ 0.09
21	3159.69 $\pm$ 0.20	3217.86 $\pm$ 0.10	3271.83 $\pm$ 0.12	3322.78 $\pm$ 0.15
22	3295.42 $\pm$ 0.21	3353.72 $\pm$ 0.19	3408.07 $\pm$ 0.19	3459.54 $\pm$ 0.42
23	3430.33 $\pm$ 0.17	3490.20 $\pm$ 0.22	3544.85 $\pm$ 0.30	-

Table 2: Frequencies and 1-σ error in (μHz) of low-l p modes for the time series spanning September 19, 1994 to February 26, 1995 as measured by the LOI.

n	l=2	l=3	l=4	l=5
15	-	2408.11 $\pm$ 0.15	2458.73 $\pm$ 0.23	2506.18 $\pm$ 0.20
16	-	2541.69 $\pm$ 0.22	2593.01 $\pm$ 0.28	2641.54 $\pm$ 0.06
17	-	2676.03 $\pm$ 0.18	2728.66 $\pm$ 0.15	2777.33 $\pm$ 0.13
18	2754.30 $\pm$ 0.12	2811.39 $\pm$ 0.16	2864.30 $\pm$ 0.09	2913.37 $\pm$ 0.22
19	2889.35 $\pm$ 0.09	2947.01 $\pm$ 0.06	3000.14 $\pm$ 0.09	3049.78 $\pm$ 0.11
20	3024.76 $\pm$ 0.19	3082.39 $\pm$ 0.11	3135.85 $\pm$ 0.11	3186.32 $\pm$ 0.12
21	3160.16 $\pm$ 0.15	3217.82 $\pm$ 0.14	3271.52 $\pm$ 0.19	3322.71 $\pm$ 0.13
22	3295.00 $\pm$ 0.14	3354.17 $\pm$ 0.19	3408.29 $\pm$ 0.15	-
23	3430.77 $\pm$ 0.16	3489.78 $\pm$ 0.22	-	-

Table 3: Sidereal a_1 component of the splitting (in nHz) for low-l p modes for the time series spanning May 2 to October 11, 1994 as measured by the LOI. The errors are 1-σ value.

n	l=2	l=3	l=4	l=5
15	-	671 $\pm$ 104	561 $\pm$ 59	482 $\pm$ 57
16	788 $\pm$ 110	354 $\pm$ 62	216 $\pm$ 75	504 $\pm$ 37
17	-	410 $\pm$ 84	434 $\pm$ 47	452 $\pm$ 31
18	396 $\pm$ 71	312 $\pm$ 52	431 $\pm$ 21	406 $\pm$ 28
19	282 $\pm$ 39	504 $\pm$ 37	423 $\pm$ 33	431 $\pm$ 23
20	428 $\pm$ 76	387 $\pm$ 44	386 $\pm$ 30	476 $\pm$ 22
21	661 $\pm$ 192	354 $\pm$ 53	505 $\pm$ 45	430 $\pm$ 48
22	743 $\pm$ 149	606 $\pm$ 94	412 $\pm$ 76	340 $\pm$ 113
23	916 $\pm$ 97	628 $\pm$ 96	491 $\pm$ 83	-
<>	428 $\pm$ 28	431 $\pm$ 19	429 $\pm$ 13	449 $\pm$ 11

Table 4: Sidereal a_1 component of the splitting (in nHz) for low-l p modes for the time series spanning September 19, 1994 to February 26, 1995 as measured by the LOI. The errors are 1-σ value.

n	l=2	l=3	l=4	l=5
15	-	357 $\pm$ 51	242 $\pm$ 128	492 $\pm$ 50
16	-	403 $\pm$ 137	317 $\pm$ 91	475 $\pm$ 21
17	-	499 $\pm$ 85	319 $\pm$ 61	390 $\pm$ 37
18	650 $\pm$ 65	445 $\pm$ 65	428 $\pm$ 29	405 $\pm$ 33
19	399 $\pm$ 58	508 $\pm$ 26	445 $\pm$ 36	434 $\pm$ 31
20	632 $\pm$ 267	393 $\pm$ 48	427 $\pm$ 42	534 $\pm$ 33
21	266 $\pm$ 121	425 $\pm$ 58	390 $\pm$ 78	482 $\pm$ 36
22	399 $\pm$ 75	397 $\pm$ 175	209 $\pm$ 78	-
23	566 $\pm$ 107	557 $\pm$ 92	-	-
<>	467 $\pm$ 35	461 $\pm$ 18	403 $\pm$ 17	460 $\pm$ 12